SYNERGY OF GREEN TEA REDUCED TAMOXIFEN-LOADED SILVER NANOPARTICLES EXHIBIT OGT DOWNREGULATION IN BREAST CANCER CELL LINE

M. RASHEED[a], A. ALI[a], S. KANWAL[b], M. ISMAIL[c], N. SABIR[d], F. AMIN[e*]
[a]*Atta ur Rehman School of Applied Biosciences, National University of Science and Technology (NUST), Islamabad, Pakistan*
[b]*Guangzhou Institutes of Biomedicine and Health, Chinese Academy of Sciences, China*
[c]*Institute of Biomedical and Genetic engineering, Islamabad, Pakistan*
[d]*Department of Physics, GC University Faisalabad, Pakistan*
[e]*School of Natural Sciences, National University of Science and Technology (NUST), Islamabad, Pakistan*

Breast cancer is the most prevalent type of cancer diagnosed in women. Current therapeutic methodologies for cancer include radiotherapy, chemotherapy and surgery. However, the major clinical obstacle in the treatment of cancer with chemotherapy is the development of *de novo* or acquired drug resistance due to ineffective drug delivery to the tumor site or the development of resistance with passage of treatment. To overcome these limitations, therapeutic nanoparticles have emerged as auspicious alternative of the conventional chemotherapy against breast cancer drug resistance and demonstrate improved efficacy with reduced adverse effects. Therefore it is important to comprehend the underpinning mechanism of nanoparticles interaction with cancer cells to figure out the lethal effect of nanoparticles on otherwise healthy cells. In this study, we synthesized therapeutic silver nanoparticles by the reduction of metal salt through tea extract in the presence of Tamoxifen. The cytotoxicity of Tamoxifen capped green tea reduced nanoparticles (TAM-AgNPs) was found to increase and the effect was co-related with decreased expression of an enzyme, called O-GlcNAc Transferase (OGT). This suggests that, OGT can be targeted as potential therapeutic candidate and a detailed activity mechanism of OGT needs to be further explored as it has role in increasing the efficacy of drug delivery.

(Received: July 30, 2018; Accepted August 19, 2019)

Keywords: Breast cancer, Cytotoxicity, Green tea, Nanoparticles, Tamoxifen

1. Introduction

About 60-70% of the breast cancer is estrogen receptor positive (ER+). ER+ breast cancer can be treated by modulating the action of ER through Tamoxifen, resulting in inhibition of tumor progression [1]. Tamoxifen has improved overall survival and has contributed to reduced breast cancer cell deaths in last decades [2]. However, 20-30% of the breast cancer patients exhibit either *de novo* or acquired resistance against Tamoxifen. Despite beneficial effects of Tamoxifen against cancer, drug resistance is one of the significant clinical problems [3]. Over the past few decades, significant advancements have been made in our fundamental treatment strategies which have been coupled with nanotechnology and in turn lead to improvement of overall diagnostic and treatment methods [4-7]. However, there has been a little exertion on the understanding of synergistic effects of different modalities.

Today a number of green and chemical routes are known for size and shape controlled synthesis of metal nanoparticles especially silver nanoparticles [7-10]. The bottom line is the reduction of metal ions through a reducing agent normally in the presence of appropriate capping

*Corresponding author: faheem_phy@yahoo.com

molecules. However, chemical methods involve chemicals which are more often volatile in nature and involve onerous steps to prepare desired particles [11]. The biological agents on the other hand are economic, abundant and benign in nature. The type and concentration of reducing agent strongly influences the size, shape and properties of the transformed nanoparticles [12-14]. The smaller size can improvise enhanced antibacterial properties owing to large surface area to volume ratio of these nanoparticles. This in turn mitigates the development of resistant strains by microbes against metal ions. Metal nanoparticles improvise more toxicity as compared to their bulk counterparts. This can be attributed to the release reactive oxygen species (ROS) such as hydrogen peroxide or metals ions from the surface of particle [15]. Therefore, indispensable need is to develop such green methods which can afford biological synthesis of nanoparticles and in turn minimize the drawbacks associated with conventional reducing agents. Among repertoire of biological sources having innate reducing properties, most notable are bacteria, fungi, actinomycetes, as well as plant extracts [16, 17]. Plant extract are advantageous as they do not require identification of potent strain, maintenance of aseptic conditions for the profuse growth of microorganisms, offering minimal infection and contamination to name a few [18].

Green tea (*Camellia Sinensis*) is known for its medicinal peculiarity, especially anti-carcinogenic activities, for a long time [19, 20]. *Camellia Sinensis* contains polyphenols and terpenoids which mimic bactericidal and antioxidant activity. The major effect has been attributed towards the polyphenol-catechins present in the green tea [5]. On the other hand, silver nanoparticles themselves are known to prelude cytotoxicity in various cell lines irrespective of synthesis method [21]. Vilchis-Nestor *et al.* used *Camellia Sinensis* simultaneously as reducing and capping agent for Au and Ag nanoclusters [22]. The authors found the particle size to increase with increasing the concentration of plant extract to metal salt ratio. Sun *et al.* evaluated the antibacterial activity of green tea-reduced AgNPs. The authors demonstrated that tea-reduced silver nanoparticles showed minimal efficacy towards antimicrobial activity by better shielding of surface thus mitigating the release of Ag ions [23].

In the present study, green tea reduced Tamoxifen-capped silver nanoparticles (TAM-AgNPs) were synthesized using reported protocols [24] with minor modification and analyzed for their synergistic anti-carcinogenic effect against breast cancer cells. The silver ions were reduced through green tea infusion in the presence of Tamoxifen. The exogenous surface of the prepared nanoparticles is highly plausible for the adsorption of guest molecules. The ethanamine moiety of Tamoxifen is believed to commensurate the nanoparticle surface and therefore controlling the size of nanoparticle [25]. The cytotoxicity of Tamoxifen-assisted nanoparticles as well as green tea assisted-Tamoxifen has already been studied [6, 26-28]. The studies showed that the potency of free Tamoxifen was enhanced by 1.3 to 2.7 fold as a result of conjugation with nanoparticle surface and therefore resulted in the increased efficacy against MCF-7 cells. The MCF-7 cell line was used as a model in our study, as it retained several characteristics of differentiated mammary epithelium, including the Estrogen receptors which respond to Tamoxifen. The potential of current system to enhance Tamoxifen viability was assessed by analyzing the genetic expression of O-GlycNAc Transferase (OGT). OGT plays a major role in O-GlycNAcylation. O-GlycNAcylation is known to increase in cancer cell lines compared to normal cell lines and enhances the invasive properties of breast cancer cells in vivo [29]. Moreover, an increased OGT expression was observed with increased tumor grade implicating that OGT may play a role in tumor progression and metastasis [30]. According to a study conducted by Kanwal et al., enhanced O-GlycNAcylation protects MCF-7 cells from Tamoxifen induced apoptosis [31].

2. Materials and methods

All the chemicals used in this study were of analytical grade. Silver nitrate, Tamoxifen and Trizol were purchased from VWR International. Plant leaves were obtained from Peshawar. MCF-7 cell line, Cell culture medium, reagents for MTT assay and DPBS were generously provided by Institute of Biomedical and Genetic Engineering, Kahuta Research Laboratories. Primers used for GAPDH and OGT genes were purchased from Eurofins genomics. Real time CYBR green kit was purchased from Thermo Scientific.

2.1 Preparation of extract

Green tea infusion was prepared by percolation method. 10g of green tea leaves were taken, washed and dried. Leaves were kept in ethanol for 48 hours at room temperature. Supernatant was collected and filtered through vacuum filtration assembly using 0.45µm pore size filter paper. Filtrate was collected and subjected to rotary evaporation below 50°C. The resultant mixture obtained is evaporated, dried, grinded and stored as powder at 4°C. The 96µM infusion was prepared by dissolving the powder in DMSO (192mg in 2mL of DMSO).

2.2 Synthesis of Tamoxifen loaded silver nanoparticles

A 100µM (12mL) solution of Tamoxifen was prepared in DMSO. 12mL of tea extract infusion and 100mL of 1mM silver nitrate solution were mixed in the presence of Tamoxifen solution (12mL). The color of solution turned slowly to brown confirming the reaction inchoation. The reaction was left stirring for 1 hr to ensure efficient mixing of all components.

2.3 Characterization

2.3.1 UV/Vis spectroscopy

Optical density was measured as a function of wavelength to verify the formation of silver nanoparticles. UV/Vis spectrophotometer (model T-60 PG instruments, UK) was used for this purpose. A diluted sample in plastic cuvette was used to avoid re-absorbance. The scanning range of sample was 200-600nm. DMSO was used as a blank.

2.3.2 Scanning electron microscopy (SEM)

SEM analysis was done using Mira 3 TESCAN instrument in order to analyze mean particle size and morphology of nanoparticles. The diluted samples were well sonicated before putting them on the grid. Single drop of each sample was dried under UV lamp for 20-30 min. The samples were sputter coated with gold to make them conductive and subsequently mounted for analysis. The metal content was quantified by using integral EDS facility in SEM instrument.

2.3.3 Atomic force microscopy (AFM)

For AFM analysis, a thin film of the sample was prepared on a glass slide by adding a drop of the sample on the slide. The slide was allowed to dry for 5 min before mounting on the analyzer. The slides were then scanned with the AFM (JOEL, Model no JSPM-5200) in the tapping mode. SPIP 6.2.8 software was used for the particle size distribution analysis.

2.3.4 Fourier Transform Infrared (FTIR)

FTIR analysis of the dried TAM-AgNPs was carried out through the potassium bromide (KBr) pellet (FTIR grade) method and spectrum was recorded using Spectrum-100, Perkin-Elmer, USA Fourier transform infrared spectrometer equipped with Infrared Microscope using transmittance mode operating in the range of 450-4000 cm^{-1} at a resolution of 1 cm^{-1}.

2.3.5 X-ray diffraction (XRD)

Powder X-ray diffraction was carried on the solution samples of TAM-AgNPs using X-ray generation device, model no. IPDS II (STOE, Germany) with Cu-K_α X-rays of wavelength (λ=1.54056 Å). The data was taken for the 2θ range of 20° to 80° with a step of 0.02°. Tamoxifen was used as a reference.

2. 4 Cell culture assay

Human breast cancer MCF-7 cell line is used as *in vitro* model for breast cancer. MCF-7 cells were grown in 25 cm^2 tissue culture flasks and were maintained in 5% CO_2 atmosphere at 37 °C. MCF-7 cell line was obtained from IBGE, KRL hospital, Islamabad. The growth medium comprised of RPMI 1640 supplemented with Earle's salts, 2mM L-glutamine, nonessential amino acids, sodium bicarbonate and 1mM sodium pyruvate, 10% v/v FBS, 100 U/mL penicillin, and 100 µg/mL streptomycin was provided. The growth medium was changed twice a week and cells were trypsinized and passaged at 80% confluency. Two set of experiments was performed in

parallel and each of these were repeated three times. First set was used for MTT assay and second for quantitative real time PCR (qRT-PCR), Exponentially growing cells were seeded at a density of 10,000 (cell/well) in triplicate of 96 well micro plates for MTT assay and cells were seeded at a density of 50,000 cells/well in triplicate of 6-well culture plate for qualitative Real time analysis.

After 24 hours of incubation, cells were treated. The treatment was categorized in three groups i.e. 1) Control cells: (no treatment). 2) Drug treated cells: (100µM concentration of Tamoxifen dissolved in DMSO). Different concentration of drug (5-40µg/mL is used in MTT assay to determine the cytotoxicity at each; 5µg/mL step. 3) TAM-AgNPs treated cells: (solution of concentration 2mg/2ml). Different concentration of TAM-AgNPs (5-40µg/mL) is used in MTT to determine the cytotoxicity at each; 5µg/mL, step.

2.5 Cytotoxicity MTT assay

Standard MTT assay was used to determine the cytotoxicity of green tea reduced Tamoxifen-capped silver nanoparticles as well as to measure their effect on MCF-7 cells. Upon completion of the incubation period, the medium was aspirated, and cells were washed with DPBS, pH 7.4. Subsequently, 150µL of MTT solution (500 µg/mL in DPBS) was added to each well and re-incubated for 3 hrs to facilitate formation of formazan crystals. The excess solution was then aspirated carefully and replaced by 100µL of DMSO and was left at room temperature for 1 hr. The color rapidly changed to purple and absorbance was recorded on the plate reader at 570nm.

2.6 RNA extraction, reverse transcription and qPCR

RNA was extracted (Abcam protocol) from all experimental groups by using Trizol reagent. Extracted RNA was resuspended in DPEC treated water and stored at -80 °C. The cDNA was synthesized by using OligodT primers that specifically bind to poly A tail of RNA. The quantity of extracted RNA and cDNA was assessed by using spectrophotometer (Thermo scientific Nano drop 2000C). The quantitative expression analysis of OGT was performed by using using SYBR green through quantitative real time PCR (qRT-PCR). Real Time PCR Detection System (Applied Biosystems 7300 sequence detection). .

The sequences of the OGT primers used in these experiments are:

Primer name	**Sequence**	**T_m**
OGTS1	TGGGCAAACATTCTGAAGCG	60.4
OGTAS1	TCCAAGCAGACATCAGCCAG	62.4

2.7 Statistical analysis

Expression of OGT was measured using above mentioned primers in three independent experiments. Results are optimized using GAPDH as housekeeping gene control in each experiment. Further Statistical analysis was done using Prism software (Graph pad). Difference in Ct of control and OGT was used and graph was drawn. Analysis was done using one way ANOVA function. Results correspond to the mean (±) SEM values of three independent experiments.

3. Results and discussion

Taxonomic and morphological features of *Camellia Sinensis* were identified by comparison to published data. Green tea powder was prepared by percolation followed by rotary evaporation, drying and grinding. 10g of leaves were taken and the resulting yield of 2.46g of extract was obtained. The powder obtained was dark green in color. Powder was dissolved in 2mL of DMSO at a concentration 96 mg/mL for further use.

Plant infusions generally contain a number of enzymes. These enzymes possess the ability to reduce ions in solution. Silver nitrate is a colorless solution at room temperature. The addition of green tea infusion instantaneously leads to a remarkable color change of the silver nitrate solution. Synthesis of AgNPs was confirmed by the color change as the reaction between silver

nitrate, plant extract and drug proceeds, the change in color of reaction mixture occurs. The color of silver nitrate solution changes from colorless to turbid green and then further turns pale green which is the signature of characteristic plasmon peak development. This change in color was obtained due to the reduction of Ag+ ions to Ag particles through the action of reducing enzymes present in extracts. UV/Vis spectroscopy gave further insight to the shape and size of nanoparticles (Figure 1). The plasmon peak of spherical silver nanoparticles ~ 420nm is in lieu with the typical value for absorbance of such silver nanoparticles. The width of plasmon peak suggests size distribution as well as the average particle size. The average particle is related to the FWHM of the absorbance peak through following relation,

$$\gamma(r) = \gamma_0 + \frac{A\vartheta_F}{r}$$

where $\gamma(r)$ is the FWHM of the absorbance peak, ϑ_F is the Fermi velocity and A is a constant attributed to scattering process (A is ¾ for silver). The average particle size calculated from UV/Vis came out to be 27.8 ± 2nm.

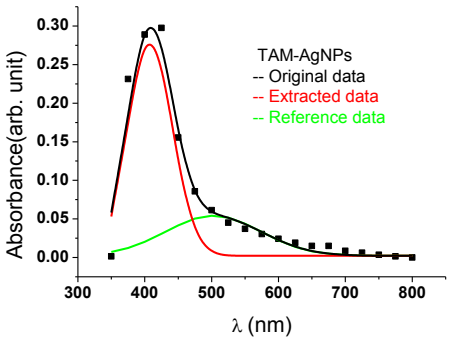

Fig. 1 UV-Visible spectroscopy of silver nanoparticles. Graph represents the UV spectrum of AgNPs synthesized by extract of green tea coupled with Tamoxifen. Y-axis represents normalized absorbance and X-axis shows the wavelength. A visible peak at 425nm represents the presence of silver AgNPs. The black line represents the original data while the green line is the extracted data for TAM-AgNPs. The green line is the reference data chosen in a way that the NPs do not absorb in this range

SEM image of silver nanoparticles is shown in Fig. 2. The morphology of the nanoparticles was found to be spherical. The average size of nanoparticles was calculated as 50nm. Energy Dispersive X-ray Spectroscopy (EDS) analysis was done for elemental analysis of the nanoparticles. The analysis was done at magnification of 90× with a pixel size of 512 × 384, keeping the probe current and voltage as 1.00000nA and 20kV. EDS analysis revealed the presence of silver (11.54%) as indicated in the graph (Fig. 3). The presence of other elements such as calcium, oxygen, Sulfur and chloride can be attributed to the presence of organic source i.e. plant extract.

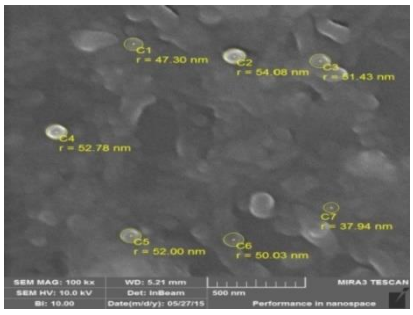

Fig. 2. Scanning Electron Microscopic image of gold plated TAM-AgNPs. The SEM image of TAM-AgNPs at 100,000× resolution depicts the uniformity of nanoparticles across the magnified section and indicating the size of nanoparticles which was found to be 50nm±3.

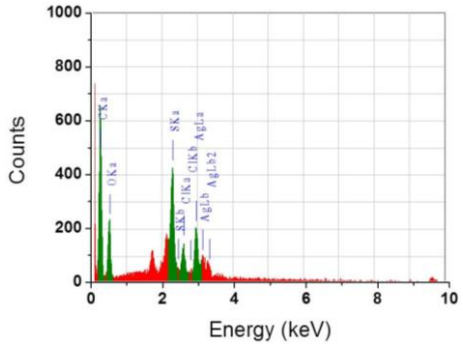

Fig. 3. Spectroscopy analysis for elemental composition determination of hybrid TAM-AgNPs. The graph shows the elemental composition of TAM-AgNPs present in colloidal solution. The presence of silver is evident by a peak at 3keV (X-axis) which confirms the formation of TAM-AgNPs

AFM analysis of TAM-AgNPs is shown in Figure 4. The analysis gives a better insight into topographical aspects of the NPs. An average size of 17.5nm with a size distribution of ±2.5nm was measured. The scanning range along X, Y and Z-axes was kept at 30µm × 30µm × 23.5nm. The incompatibility between the particle size as calculated by UV-Vis spectroscopy, SEM and AFM can be attributed to the fact that the high accelerating voltage like 20keV in case of SEM reveals more lateral aspects while AFM adheres to surface information. In the case of UV-Vis spectroscopy the sources of error are even more pronounced as the scattering can be from big clusters as well the complicated data analysis.

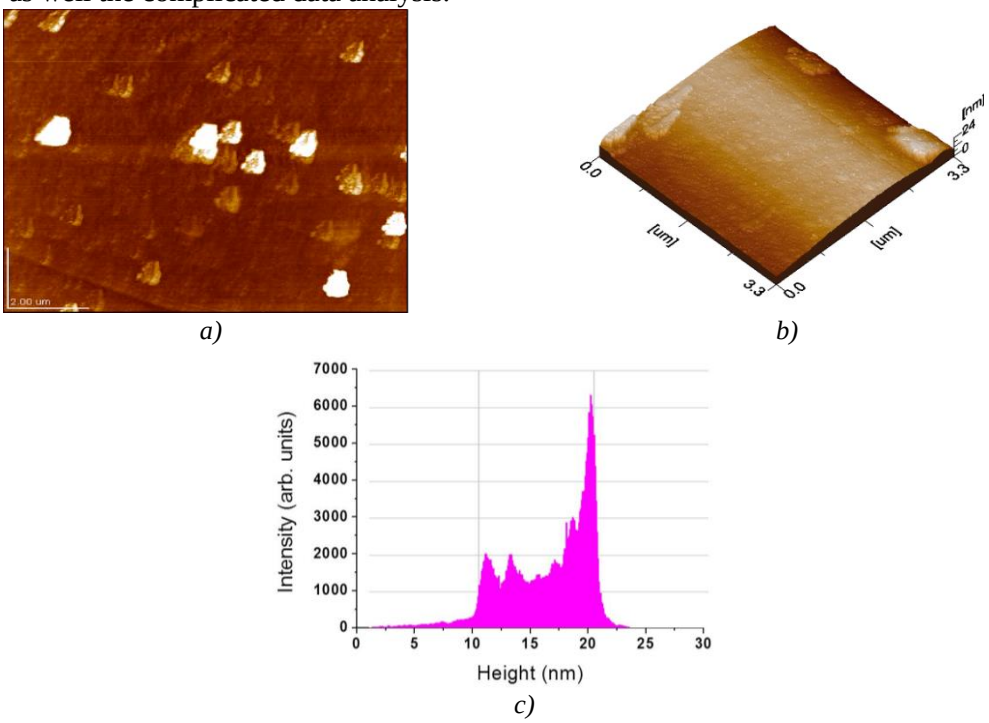

Fig. 4. Atomic Force microscopy images for size distribution of TAM-AgNPs films. (A) Represents the 2D (XY scan) AFM image of nanoparticles showing color mapping. (B) Represents the 3D topographical image of nanoparticles showing the size of nanoparticles. (C) Represents the histogram indicating the size distribution of nanoparticles and shows that the mean size range is between 17.5 ± 2.5 nm

FTIR analysis was performed to determine the contribution of chemically active functional groups involved in reduction of silver nitrate. FTIR analysis of green tea extract, Tamoxifen and Tamoxifen capped silver nanoparticles was carried out for a comparative analysis. Shift in the

chemical groups was analyzed as a function of reducing and capping agents for nanoparticles. Peaks were analyzed through Essential FTIR using 3.50 build 32 built software. Common peaks and band shifts before and after the synthesis of nanoparticles are shown in the Figure 5. The band at 3429-3436 cm^{-1} is due to stretching vibrations of hydroxyl group in water and alcohols and to N–H stretching in amines. The peaks at 2916, 2929 and (2915, 2856) cm^{-1} C–H (m or s) in tea extract, Tamoxifen and TAM-AgNPs respectively stretch in alkanes while the peak at 3002 and 2767 cm^{-1} in tea extract and Tamoxifen correspond to O–H stretch in carboxylic acid. The peaks at 1652, (1511, 1609) and 1646 cm^{-1} in tea extract, Tamoxifen and TAM-AgNPs respectively, correspond to C=C (m, m) stretch in aromatic ring or C=O stretch in polyphenols. The bands 1435 and 1436 cm^{-1} in tea extract and TAM-AgNPs are assigned to in plane bending C-H vibrations. The band at 1246 cm^{-1} in Tamoxifen is attributed to the C-O-C vibrations. The C-N stretch in aliphatic amines and asymmetrical C–O stretching in amino acid causes band at 1024, 1031, 1029 cm^{-1} in tea extract, Tamoxifen and TAM-AgNPs respectively. Finally the band at 706, 699, 702 cm^{-1} in tea extract, Tamoxifen and TAM-AgNPs respectively, is the result of C–H out of plane bending in aromatic ring. Thus by looking at the IR spectrum it can be claimed that polyphenols in green tea (broad peak around 3430 cm^{-1}) participate actively in the reduction of silver ions while Tamoxifen adheres to the surface of nanoparticle via its ethanamine moiety as N-H stretching in Tamoxifen lies more closely to the NP peak at 3436 cm^{-1}. Another interesting aspect is damping of few modes e.g. C-H stretching at 1024 and 964 cm^{-1} in case of tea extract to 1029 and 970 cm^{-1} in case of TAM-NPs which may be attributed to the tight bonding of aliphatic chains on the surface of NP.

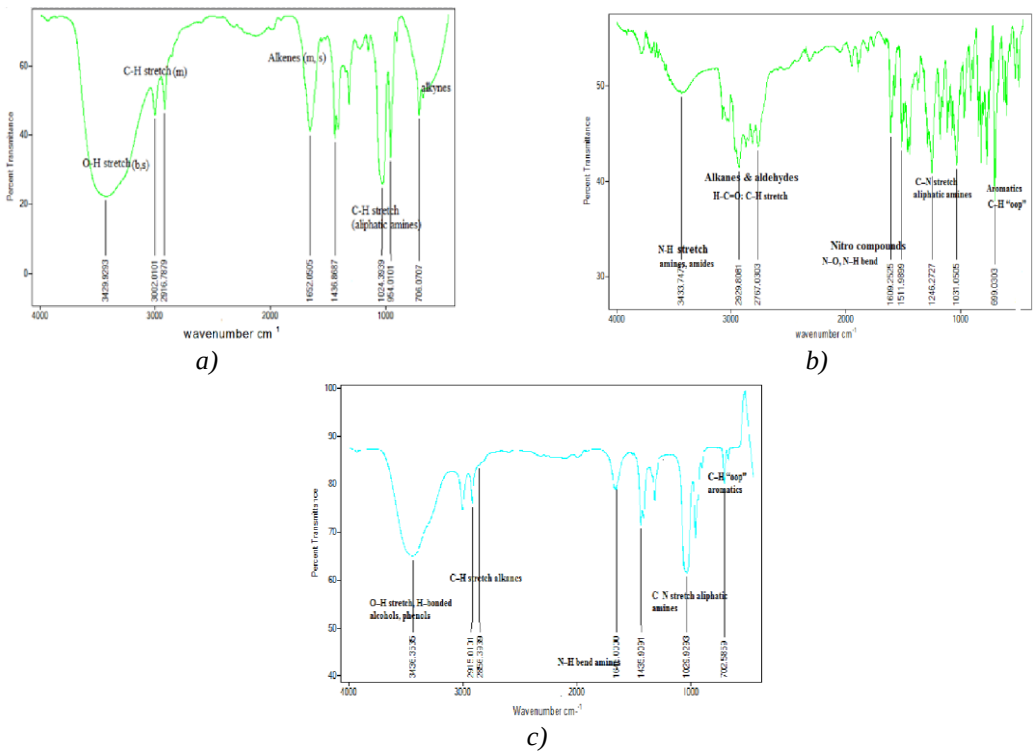

Fig. 5. FTIR spectrographs for the evaluation of surface groups on AgNPs. (A) Represents the spectrum of Green tea extract. (B) Shows spectrum of 99% pure Tamoxifen. (C) Shows Tamoxifen capped silver nanoparticles.

The XRD pattern of nanoparticles exhibit different peaks which confirmed the crystalline nature of NPs. For this purpose, a drop of sample was dried on a glass slide. The sample was prepared as a thin film. Due to the small amount of available sample a much diluted layer was deposited on the slide. Figure 6 shows the XRD spectrum of TAM-AgNPs. The diffraction peaks at 2θ = 38.19, 44.315, 64.775 and 77.5 can be indexed to (111), (200), (220) and (311) planes of

pure silver (FCC) while various peaks including (112), (103) between 20-32° correspond to presence of Tamoxifen. Lack of hkl planes for all peaks could be described on the basis that organic material didn't show good response to XRD and (hkl) values report can't be generated due to software restriction. The Tamoxifen was used as a reference (spectra not included).

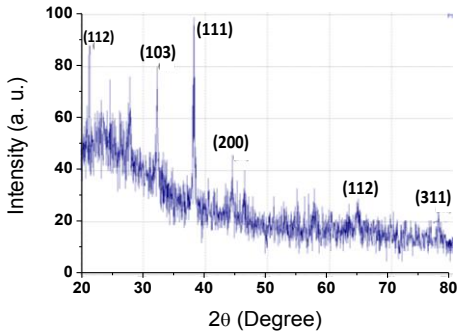

Fig. 6. Graph representing the XRD pattern of AgNPs with both the integrated peaks of silver and Tamoxifen at 2θ plane. The peaks (111), (200), (311) correspond to the FCC structured silver

3.1 MTT assay

Cytotoxicity of nanoparticles was tested against MCF-7 estrogen receptor positive (ER+) breast cancer cell line. It was found that the cell viability (inverse percentage cytotoxicity) decreased with increasing concentration of TAM-AgNPs (Figure 7). The applied dose was increased at various intervals of 5µg/mL up to a maximum of 40µg/mL. Both green tea and Tamoxifen were also tested in the same concentration range for their cytotoxicity against MCF-7 cell line as a control. The cytotoxicity of TAM-AgNPs was higher than that of Tamoxifen alone. It was found that the cytotoxicity enhances 1.7 fold as compared to free Tamoxifen which is again in line with the reported literature [22]. The possible mechanism underlying the enhanced efficacy of TAM-AgNPs against breast cancer cells may refer to the enhanced drug accumulation and sustained action of nanoparticles as compared to a single dose of free drug. Furthermore it shows that the effect is merely due to the drug and not the nanoparticles.

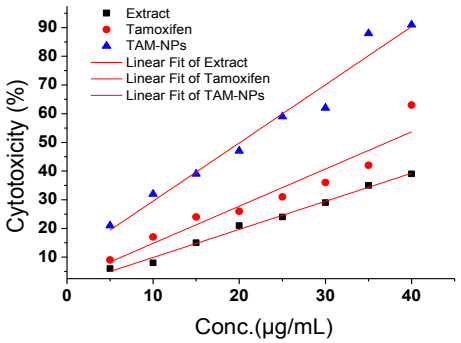

Fig. 7. Cytotoxic effects of Tamoxifen, extract and TAM-AgNPs on MCF-7 cells. Cells were treated individually with all the three agents at 5-40 µg/mL concentration. The results represent that highest cytotoxic potential has been attributed by TAM-AgNPs

3.2 Real time PCR analysis

OGT expression was quantified at mRNA level through quantitative real time PCR analysis by using specific primers and it was normalized by using housekeeping gene GAPDH as control. Results showed that the OGT expression was decreased by treatment of cells with Tamoxifen and this effect is further enhanced when cells were treated with TNPs (Fig. 8). This result is the mean of three independent experiments and error bars represent the standard error of

the mean. Statistical analysis was carried out by using one-way ANOVA test which resulted in significant decrease of OGT expression with Tamoxifen treatment compared to control and importantly this effect was further aggravated with TNPs. These result showed that OGT may have the potential to be targeted for cancer therapeutics. Moreover, green tea reduced Tamoxifen capped silver nanoparticles may act as an effective anti-breast cancer agent.

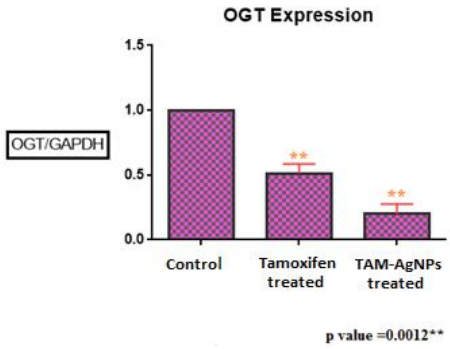

Fig. 8. Differential OGT expression by real time PCR analysis. Graph with different treatments at X-axis shows that OGT level decreased about 2 fold when treated with Tamoxifen and 4 fold when treated with TAM-AgNPs. The result represents the mean of three independent experiments and error bars represent the standard error of the mean. Treated groups showed statistically significant differences from the control group by the one-way ANOVA test (p=0.0012). The p-value suggests that the results are highly significant

4. Conclusions

Green tea reduced Tamoxifen-capped silver nanoparticles, has been successfully developed in this study. The results show that the synthesized nanoparticles have narrow size distribution and they exhibit synergy with Tamoxifen against breast cancer cell line. The synergetic effect shown is potentially due to decreased OGT expression. The synthesized nanoparticles however needed to be scrutinized for their colloidal stability. Our previous study (Kanwal et al., 2013) showed that the increased expression of OGT is involved in inducing Tamoxifen resistance in MCF-7 cells. Thus, it suggests that targeting OGT can be considered as one of therapeutic strategies. Here, in this study we showed that Tamoxifen treatment decreased expression of OGT which was further decreased with TNPs. This provides us a new direction of research to consider the use of nanoparticles to decrease expression of OGT which may result in decreasing aggravation of cancer and it may also sensitize the cells for cancer therapeutic agents. Therefore, we also need to explore the effect of such nanoparticles capped drugs to target different oncogenes.

Acknowledgements

The authors are thankful to Higher Education Pakistan for financial assistance. SNS, SCME and ASAB (National University of Sciences and Technology, Islamabad, Pakistan) as well as KRL are acknowledged for different facilities.

References

[1] A. Jemal, F. Bray, M. M. Centre, J. Ferlay, E. Ward, D. Forman, CA Canc. J. Clinicians, **61**(2), 69 (2011).
[2] A. Errico, Nat. Rev. Clin. Oncol. **12**, 66 (2015).
[3] V. C. Jordan, B. W. O'Malley, J. Clin. Oncol. **25**(36), 5815 (2007).
[4] A. Sharma, A. K. Goyal, G. Rath, J. Drug Targ. **26**(8), 617 (2018).

[5] Y. Shirakami, M. Shimizu, H. Moriwaki, Curr. Drug Targ. **13**(14), 1842 (2012).
[6] E. C. Dreaden, S. C. Mwakwari, Q. H. Sodji, A. K. Oyelere, M. A. El-Sayed, Bioconjug. Chem. **20**(12), 2247 (2009).
[7] V. Castro-Aceituno, S. Ahn, S. Y. Simu, P. Singh, R. Mathiyalagan, H. A. Lee, D. C. Yang, Biomed Pharmaco. **84**, 158 (2016).
[8] M. Wuithschick, B. Paul, R. Bienert, A. Sarfraz, U. Vainio, M. Michael Sztucki, R. Kraehnert, P. Strasser, K. Rademann, F. Emmerling, J. Polte, Chem Mater. 25, 4679 (2013).
[9] M. Grzelczak, J. Pérez-Juste, P. Mulvaney, L. M. Liz-Marzán, Chem Soc Rev. **37**, 1783 (2008).
[10] S. P. Chandran, M. Chaudhary, R. Pasricha, A. Ahmad, M. Sastry, Biotechnol Prog. **22**(2), 577 (2006).
[11] F. Amin, d. Yushchenko, J. M. Montenegro, W. J. Parak, Chemphys. Chem. **13**(4), 1030 (2012).
[12] S. Agnihotri, S. Mukherji, S. Mukherji, RSC Adv. **4**, 3974 (2014).
[13] Y. Sun, Y. Xia, Science **298**, 2176 (2002).
[14] E. Caballero-Díaz, C. Pfeiffer, L. Kastl, P. Rivera-Gil, B. Simonet, M. Valcárcel, J. Jiménez-Lamana, F. Laborda, W. J. Parak, Part. Syst. Charact. **30**(12), 1079 (2013).
[15] C. Batchelor-McAuley, K. Tschulik, C. C. M. Neumann, E. Laborda, R. G. Compton, Int. J. Electrochem. Sci**. 9**, 1132 (2014).
[16] Y. Y, Loo, B. W.; Nishibuchi, M. Son, S. Radu, Camellia Sinensis. Int. J. Nanomed. 7, 4263 (2012).
[17] F. Cataldo, Eur Chem Bull. **3**(3), 280 (2014).
[18] A. K. Mittal, Y. Chisti, U. C. Banerjee, Biotech Adv. **31**(2), 346 (2013).
[19] P. Namita, R. Mukesh, K. J. Vijay, Glob. J. Pharm. **6**(2), 52 (2012).
[20] Y. C. Wang, U. Bachrach, Amino Acids **22**(2), 131 (2002).
[21] R. de Lima, A. B. Seabra, N. Durán, J. Appl. Toxicol. **32**, 867 (2012).
[22] A. R. Vilchis-Nestor, V. Sánchez-Mendieta, M. A. Camacho-López, R. M. Gómez-Espinosa, M. A. Camacho-López, J. A. Arenas-Alatorre, Mat. Lett. **62**, 3103 (2008).
[23] Q. Sun, X. Cai, J. Li, M. Zheng, Z. Chen, C.-P. Yu, Col. Surf A: Physicochem. Eng. Asp. **444**, 226 (2014).
[24] Y. Y. Loo, B. W. Chieng, M. Nishibuchi, S. Radu, Int. J. Nanomed. **7**, 4263 (2012).
[25] L. F. Gorup, E. Longo, E. R. Leite, E. R. Camargo, J. Col. Int. Sci. **360**(2), 355 (2011).
[26] S. N. Ostad, S. Dehnad, Z. E. Nazari, S. F. Fini, N. Mokhtari, M. Shakibaie, A. R. Shahverdi, Avicenna J. Med. Biotech. **2**(4), 187 (2010).
[27] R. Maji, N. S. Dey, B. S. Satapathy, B. Mukherjee, S. Mondal, Int. J. Nanomed. **9**, 3107 (2014).
[28] M. Suganuma, A. Saha, H. Fujiki, Canc. Sci. **102**(2), 317 (2011).
[29] A. Krześlak, E. Forma, M. Bernaciak, H. Romanowicz, M. Brys, Cli. Exp. Med. **12**(1), 61 (2012)
[30] S. A. Caldwell, S. R. Jackson, K. S. Shahriari, T. P. Lynch, G. Sethi, S. Walker, K. Vosseller, M. J. Reginato, Oncogene **29**(19), 2831 (2010).
[31] S. Kanwal, Y. Fardini, P. Pagesy, T. N'Tumba-Byn, C. Pierre-Eugène, E. Masson, C. Hampe, T. Issad, PLoS ONE **8**(7), 2013: e69150. doi:10.1371/journal.pone.0069150.